Journal of the Serbian Chemical Society
JSCS@tmf.bg.ac.rs • www.shd.org.rs/JSCS
J. Serb. Chem. Soc. *89* (6) 823–840 (2024)
JSCS–5758
Original scientific paper
Published 30 June 2024

Thermochemistry of pyrolyzed rutin and its esters prepared from facile biocatalytic route

NURUL NADIAH ABD RAZAK[1,2] and MOHAMAD SUFFIAN MOHAMAD ANNUAR[3]*

[1]*Centre for Foundation Studies in Science, Universiti Malaya, 50603 Kuala Lumpur, Malaysia,* [2]*School of Bioscience, Faculty of Pharmacy and Biomedical Sciences, MAHSA University, Bandar Saujana Putra, Jenjarom, Selangor, Malaysia and* [3]*Institute of Biological Sciences, Faculty of Science, Universiti Malaya, 50603 Kuala Lumpur, Malaysia*

(Received 24 June, revised 27 September 2023, accepted 2 January 2024)

Abstract: Pyrolysis of quercetin-3-*O*-rutinoside or rutin and its esters were investigated. Purified ester samples were prepared from lipase-catalyzed esterification of the parent flavonoid, *i.e.*, rutin using acyl donors with different carbon chain length. X-ray diffraction revealed the presence of crystalline peaks in the rutin esters. The degradation activation energies (E_a) as a function of conversion degree α were determined using Kissinger–Akahira–Sunose and Flynn–Wall–Ozawa methods, with corroborative results. Disparity in E_a implies distinct thermal degradation routes. For all studied compounds, degradation is a non-spontaneous process. The presence of acyl moieties and their corresponding carbon chain length in relation to thermodegradation profiles, E_a, entropy (ΔS) and enthalpy (ΔH) changes of the pyrolysis are discussed.

Keywords: activation energy; ester; flavonoid; pyrolysis; thermogravimetry.

INTRODUCTION

Quercetin-3-*O*-rutinoside, or known simply as rutin is a flavonoid with 3--hydroxyflavone backbone comprising of quercetin and disaccharide rutinose (glucose and rhamnose). Rutin is well known for its powerful antioxidant properties[1,2] alongside multiple pharmacological activities that include anti-inflammatory,[3,4] anti-diabetic[5] and anti-leukemia.[6] It has been shown that rutin preparation as a highly purified nanocrystal significantly improved its physicochemical properties, particularly its oral bioavailability.[7]

The potential of flavonoids in theranostic application is limited by their low stability and solubility in the fatty- and aqueous milieu, respectively. To circumvent a number of disadvantages in the traditional chemical synthesis, employing lipase-catalyzed acylation of flavonoid with fatty acid is highly precise for intro-

* Corresponding author. E-mail: suffian_annuar@um.edu.my
https://doi.org/10.2298/JSC230624002A

ducing non-polar group to the former. Enzymatic acylation of flavonoids has been reviewed by the previous literature.[8–10] The reaction is affected by crucial variables such as acyl donor, acyl acceptor, ratios of reactants, and nature of solvent, temperature, reaction time and water content.

Among the flavonoids, there is a strong interest in the synthesis of rutin esters as they possess wide biological activities and pharmacological effects. Rutin esters exhibit higher antioxidant properties in the various experimental conditions studied,[11–13] protect LDL cholesterol from oxidation *in vitro*,[14] inhibit sarco/endoplasmic reticulum Ca^{2+}-ATPase activity,[15] induce the significantly higher levels of micronuclei[16] and decrease the production of vascular endothelial growth factor in human K562 lymphoblastoma cells.[17] Recently, Cardona *et al.* demonstrated that rutin fatty ester formulation with 10 % poly [dimethylsiloxane-*co*-(3-(2-(2-hydroxyethoxy)ethoxy)propyl]methylsiloxane] (PDMSHEPMS) showed significant increase in mucus permeation compared to the formulation without when tested in self-emulsifying delivery system (SEDDS) for oral administration.[18] Researches have shown that rutin esters can be potentially applied in the pharmaceutical, food and cosmetic industries.[8–10]

In this study, rutin esters were synthesized *via* optimized lipase-mediated esterification of rutin, followed by their subsequent isolation to obtain analytical quantity of purified compounds for thermogravimetric studies. X-ray diffraction (XRD) was employed to study the crystallinity properties of purified rutin esters *viz.* rutin laurate, rutin myristate, rutin palmitate relative to the parent molecule, *i.e.*, rutin, along with their thermal degradation attributes; addressing an important gap in the literature on the pyrolysis of high value flavonoids and their fatty acid esters. Kissinger–Akahira–Sunose (KAS) and Flynn–Wall–Ozawa (FWO) methods were adopted to calculate the activation energies associated with calorimetric investigation of rutin and its esters. The findings provide insights on thermal degradation behavior of these valuable compounds; aiding product development alongside potential processing routes for the flavonoid esters.

EXPERIMENTAL

Materials

Lipase from *Candida antarctica* immobilized on acrylic resin (CAL-B), molecular sieve 4 Å, and the acyl acceptor, rutin were purchased from Sigma–Aldrich. Acyl donors *viz.* lauric acid (dodecanoic acid), myristic acid (tetradecanoic acid) and palmitic (hexadecanoic acid), acetone, ammonium formate, methanol and acetic acid were supplied by Merck. Analytical grade solvents and reagents were used as received.

Enzymatic synthesis of rutin ester

The reaction conditions are adopted from the earlier work.[19] Three different carbon chain lengths of acyl donor are selected, *i.e.*, lauric acid (C-12), myristic acid (C-14) and palmitic acid (C-16) for esterification. Filtered rutin (5×10^{-3} M) and fatty acid (0.25 M) were solubilized in 5 mL acetone previously dried with 4 Å molecular sieves. Direct esterification was

started by the addition of 50 mg of immobilized lipase. The reaction was carried out in screw--capped glass tubes shaken horizontally at 200 rpm, 55 °C. After 96 h, 0.2 mL aliquot from the reaction mixture was sampled. Each sample was dried at 70 °C, and re-suspended in 1 mL of methanol and filtered through a 0.22 μm PTFE filter for subsequent analysis by HPLC. Three independent replicates were made for every measurement. Control experiments (without catalyst) were also conducted in parallel.

In order to study the effects of selected reaction parameters, experimental design using full factorial design (FFD) was devised in MINITAB® 15 software. The effects of three key variables *viz.* acyl donor concentration (M, represented by lauric acid), temperature (°C) and enzyme loading (g) were initially screened using full factorial design (FFD). Lipase-catalyzed synthesis of rutin ester was performed in random triplicates with lowest, middle and highest factor levels (Supplementary material to this paper, Table S-I). The effects of studied variables were evaluated in terms of rutin ester yield as the response output.

With three variables, each studied at three levels (minimum, middle and maximum point values), there were 27 experimental runs including triplicates generated by MINITAB® 15 software. The design was completely randomized along with the sampling.

High performance liquid chromatography (HPLC)

Quantitative analysis of rutin and its esters were performed in a HPLC (Jasco, Japan) system equipped with degasser (DG 980 50), binary pump (PU 980), auto sampler (AS 950), column oven (CO 965) and ultraviolet (UV) detector (UV 975). The detector was operated in ultraviolet wavelength detection at 280 nm. A Chromolith® HR RP-18^e column (4.6 mm×10 mm, 2 μm, Merck, Darmstadt, Germany) fitted with analytical guard column (4.6 mm×10 mm×2 μm) was used for separation. The temperature of the column was maintained at 35 °C with a flow-rate of 1 mL min^{-1}. The injection volume was set at 20 μL. The separation of different components of the reaction mixture was performed using a gradient of methanol (A) and water with 0.1 % acetic acid (B) (A/B volume fraction): 0.1 (30/70), 5.0 (100/0), 10.0 (100/0), 11.0 (30/70) and 15.0 min (30/70). The conversion of reactants to acylated flavonoid (rutin ester) was calculated as the percentage difference between initial and residual molar concentration of rutin parent molecule:

$$\text{Conversion } (\%) = 100 \frac{F_{\text{initial}} - F_{\text{residual}}}{[F]_{\text{initial}}} \quad (1)$$

where $[F]_{\text{initial}}$ is the initial rutin concentration and $[F]_{\text{residual}}$ is the residual rutin concentration in the mixture at the end of the reaction. Calibration plot for rutin was constructed using its standard compound dissolved at different molar concentrations in methanol.

The pure rutin esters (rutin laurate, rutin myristate and rutin palmitate) were separated in Agilent HPLC, LC 1200 (Agilent Technologies, USA) system equipped with automatic fraction collector. The operating details for the separation of the mixtures are similar with earlier mentioned method.

Liquid chromatography/tandem mass spectrometry (LC/MS/MS)

Molecular weight analyses for rutin and its esters were performed using a liquid chromatograph (LC, Shimadzu, LC 20 AD, binary pump) interfaced to AB Sciex 3200QTrap LC/MS/ /MS with Perkin Elmer FX 15 uHPLC system used for integration, calibration, plotting of LC–MS spectra and data processing, for both qualitative and quantitative analyses. A Phenomenex Aqua C18 reversed phase column (50 mm×20 mm, 5 μm particle size) was installed as the stationary phase. Reaction components separation were achieved using different gradients

of 0.1 % formic acid and 5 mM ammonium formate in water (C) and acetonitrile with 0.1 % formic acid and 5 mM ammonium formate (D) as follows (C/D volume fraction): 0.01 (90/10), 8.00 (10/90), 11.00 (10/90), 11.10 (90/10) and 15.00 min (90/10) at a constant flow rate of 0.25 mL min^{-1}. The column oven temperature was operated at 40 °C with the injection volume of 20 μL over the total running time of 15 min. The mass spectrometer was operated in the negative turbo ion spray (ESI) mode, and the electrospray source parameters were fixed as follows: electrospray capillary voltage 3.5 kV, source temperature 500 °C. Nitrogen was used in the electrospray ionization source. The de-solvation gas and source gas flows were at 40 psi. The de-clustering potential and entrance potential were at 40 and 10 V, respectively.

Thermogravimetric analysis (TGA)

Thermal properties of standard rutin and acylated rutin *viz.* rutin laurate, rutin myristate, rutin palmitate were determined using thermogravimetric analysis (TGA) performed using Perkin Elmer TGA 4000 machine (Perkin Elmer, USA). Approximately 8 to 10 mg of the sample was loaded onto the ceramic crucible pan. Each sample was heated from 30 to 800 °C at multiple heating rates of 5, 10, 15 and 20 °C min^{-1} under a nitrogen flow rate of 20 mL min^{-1}.

Thermodynamic and kinetic analyses of thermal degradation of rutin and its esters

The activation energy (E_a) values for thermal degradation of rutin and its esters were calculated using iso-conversional method on the basis that the reaction rate depends on temperature and conversion degree. Compared to model-fitting method, the kinetic approach is preferable as it is sufficiently flexible to allow for any changes in the mechanism during the reaction course, and mass transfer limitation is minimized by the use of multiple heating rates. Two kinetic methods namely Kissinger–Akahira–Sunose (KAS) and Flynn–Wall–Ozawa (FWO) were applied for the analysis of samples thermograms. Mathematical basis and derivation for the analysis are provided in the Supplementary material.

X-ray diffraction (XRD) analysis

Powder X-ray diffraction (XRD) analysis was performed on the prepared sample powder for phase identification and determination of crystallite size using a PANalytical EMPYREAN machine (Analytical, Almelo, Netherlands). The operation voltage and current were at 40 kV and 40 mA, respectively, with a diffraction angle from 10 to 70° applying a resolution of 2θ.

The average crystallite size is determined using Debye–Scherrer equation:

$$D = \frac{\kappa\lambda}{\beta\cos\theta} \tag{2}$$

where D is mean crystallite size, κ is coefficient equal to 0.94, λ is the wavelength of the X-ray radiation used (0.15406 nm), β is full width half maximum intensity measured in radian and θ is the angle from the corrected position.

RESULTS AND DISCUSSION

Liquid chromatography/tandem mass spectrometry (LC/MS/MS)

LC/MS/MS spectra show that a single ester product is formed by the esterification of each aliphatic fatty acids (Supplementary material, Fig. S-1a–d). From the representative spectrum, a distinct signal at m/z 791.4 (t_R = 9.64 min) establishes that only a single lauric acid is acylated to each molecule of rutin to yield rutin laurate (Fig. S-1b). It is also observed that longer carbon chain length

of the acyl donor used in the reaction results in longer retention time for the acylated flavonoid, and correspondingly larger *m*/*z* value. Individual peak for rutin myristate appears at *m*/*z* of 819.5 (t_R = 10.85 min, Fig. S-1c); rutin palmitate presents its major ion peak at *m*/*z* 848.8 (t_R = 12.27 min, Fig. S-1d). For each synthesized rutin ester, consistent fragmentation pattern is evident at *m*/*z* 463.2 and 591.4 authenticating successful esterification of acyl donor molecule to the rutin parent molecule. The exact position of the esterification in rutin molecule has been authenticated from our previous study, *i.e.*, acylation by the lipase enzyme takes place specifically on the secondary 4‴-OH group of the rhamnose moiety.[19]

Effects of acyl donor carbon chain length on conversion yield

The effects of carbon-chain length of acyl donors on the lipase-mediated esterification of rutin were investigated using aliphatic fatty acids with carbon number ranging from 12 to 16. The progress of esterification reaction was monitored for 120 h, which also included the equilibrium state. The amount of synthesized rutin esters increased with reaction time. However, after 96 h, negligible changes in the rutin ester concentration was observed attributed to the significant amount of water product present in the reaction mixture (data not shown). At equilibrium, comparable conversion and reaction rate were achieved for the three types of rutin esters synthesized (Supplementary material, Fig. S-2). Similar findings are reported in the literature that showed the fatty acid chain length had a slight effect or no significant effect on conversion yield when fatty acids, of medium and high chain length, are used in acetone media.[17,20] However, Viskupicova *et al.*[11] and Ardhaoui *et al.*[21] reported that increasing the carbon number of the aliphatic fatty acids (from C12 up to C18) resulted in gradual decrease in conversion yield of esters with steric hindrance and was suggested as the primary reason. Therefore, the effect of the chain length of the fatty acid (the acyl donor) on esterification yield is difficult to generalize and remains a matter of discussion.[9]

Statistical experimental design of lipase-mediated esterification

From the three acyl donors tested (C12–C16), the esterification of rutin with lauric acid was selected as a model reaction. The effects of selected variables namely lauric acid concentration (M, factor A), enzyme loading (g, factor B) and temperature (°C, factor C) were initially screened using a full factorial design (FFD). A total of 27 experimental runs were generated, and the equilibrium concentration of rutin laurate was assayed at 96 h. Responses for variables screening experiments are shown in Table S-II (Supplementary material). The highest rutin laurate molar concentration was observed when the concentration of lauric acid, enzyme loading and temperature were specified at 0.25 M, 0.05 g and 55 °C, res-

pectively. Conversely, the lowest rutin laurate molar concentration was obtained at the lowest level of each variables when in combination. Detailed analysis of the statistical experimental design results and optimization are provided in the Supplementary material.

X-ray diffraction (XRD)

X-ray diffraction patterns of rutin and its esters are shown in Fig. S-3 (Supplementary material). The diffraction pattern provides important information on material crystallinity including its relative difference to amorphous structure. The average crystallite size of rutin and its corresponding esters are shown in Table I.

TABLE I. Determination of crystallite size using Debye–Scherrer equation; *FWHM*: full-width-at-half maximum; *D*: diameter

Sample	2θ / °	FWHM / °	*D* / nm
Rutin	15.01	0.3070	27.26
	16.84	0.2558	32.79
	22.24	0.3070	27.54
	26.29	0.2558	33.31
Rutin laurate (R-12)	5.76	0.2047	40.59
	6.79	0.2047	40.61
	9.23	0.3070	27.12
	23.03	0.2558	33.10
Rutin myristate (R-14)	5.74	0.2047	40.59
	6.74	0.2047	40.60
	9.14	0.2558	32.54
	23.03	0.2047	41.37
Rutin palmitate (R-16)	5.64	0.2047	40.58
	6.65	0.3070	27.07
	9.00	0.4093	20.35
	22.63	0.2047	41.37

Rutin exhibits intense and sharp diffraction peaks at 2θ 15.01, 16.83, 22.3 and 26.2° with crystallite size of 27.27, 32.79, 27.54 and 33.31 nm respectively. These results are comparable and consistent with Şamlı *et al.* demonstrating the crystalline behavior of rutin.[22] On the other hand, X-ray diffraction of rutin esters shift towards lower angles and exhibit similar pattern at 5.76, 6.79, 9.23 and 23.03° for rutin laurate, 5.74, 6.74, 9.14 and 23.03° for rutin myristate and 5.64, 6.65, 9.00 and 22.63° for rutin palmitate. At 2θ 5.64 to 5.76°, for all studied esters, equal crystallite size is determined. Sharp peaks in diffractograms of pure rutin and its corresponding esters specify crystalline behavior of the compounds.

The peak top position of rutin 2θ 26.2° shifts to lower angle (2θ 26.2 to 23°) for the corresponding esters with the same peak intensity values. Interestingly, at this angle, comparable crystallite size (33.31 nm) is observed for rutin and rutin

laurate. However, the crystallite size increases from 33.31 (for rutin) to 41.37 nm (for rutin myristate and rutin palmitate). While minor differences are observed in the diffractograms, it categorically excludes possible dramatic alteration in the crystallinity of the samples. It can be concluded that the presence of fatty acid moiety in the rutin ester results in similar crystalline behavior as in pure rutin, and the average size of crystallite is proportional to acyl donor chain length. The esterification of fatty acids with higher chain lengths, such as myristic acid and palmitic acid, disrupts intermolecular hydrogen bonds, leading to the formation of an ordered and compact molecular arrangement and consequently altering the crystalline size of rutin. Similar pattern is observed in the modification of maize starch by esterification with fatty acid moieties.[23] This is further supported by the entropy change values of rutin ester showing increase in orderliness with the increase of fatty acid length (ΔS, Table IV). In general, crystalline substances are physically more stable relative to amorphous ones since their molecules are arranged in a highly ordered, regular pattern.

Thermogravimetric analysis (TGA)

In this study, TGA was used to investigate the thermal behavior of rutin and its corresponding esters. While most thermal degradation studies of rutin and other flavonoids are associated with the thermal treatment of samples,[24–26] there is a noticeable gap in the literature concerning the use of TGA. Weight loss curve provides the information to analyze the changes in sample composition and its thermal stability. First derivative of the curve for a particular sample in relation to changes in temperature is used to show the point at which weight loss is most evident. TG and DTG curves for thermal degradation of rutin and its esters are shown in Fig. 1, and the corresponding data are summarized in Table II.

TG and DTG curves show the degradation of rutin and its corresponding esters occurring in four stages, indicating a complex process with multiple stages (Fig. 1). Although the curves are not radically dissimilar, observable differences for thermograms of rutin and its esters are apparent.

The weight of rutin parent molecule decreases gradually within the range of 30–200 °C, with a mass loss of about 6 %. Using pure rutin compound as a reference, the first degradation stage of rutin esters shifts towards lower temperature. TG curves of rutin esters exhibit initial weight loss of 6–8 % in the temperature range of 30–90 °C (Fig. 1a). The mass loss below 90 °C of rutin laurate is lower than rutin myristate and palmitate (Fig. 1b). For all samples, a small region of weight loss around 100 °C can be seen from their corresponding DTG curves attributed to the evaporation of moisture (Fig. 1b). According to da Costa *et al.* the loss of water molecules (dehydration) of rutin occurs in the first two stages involving molecular rearrangement of rutin polymorphic structure.[27]

With increasing temperature, small molecule and weak chemical bonds gradually decompose and TG curves fall away. It is observed that the first and sec-

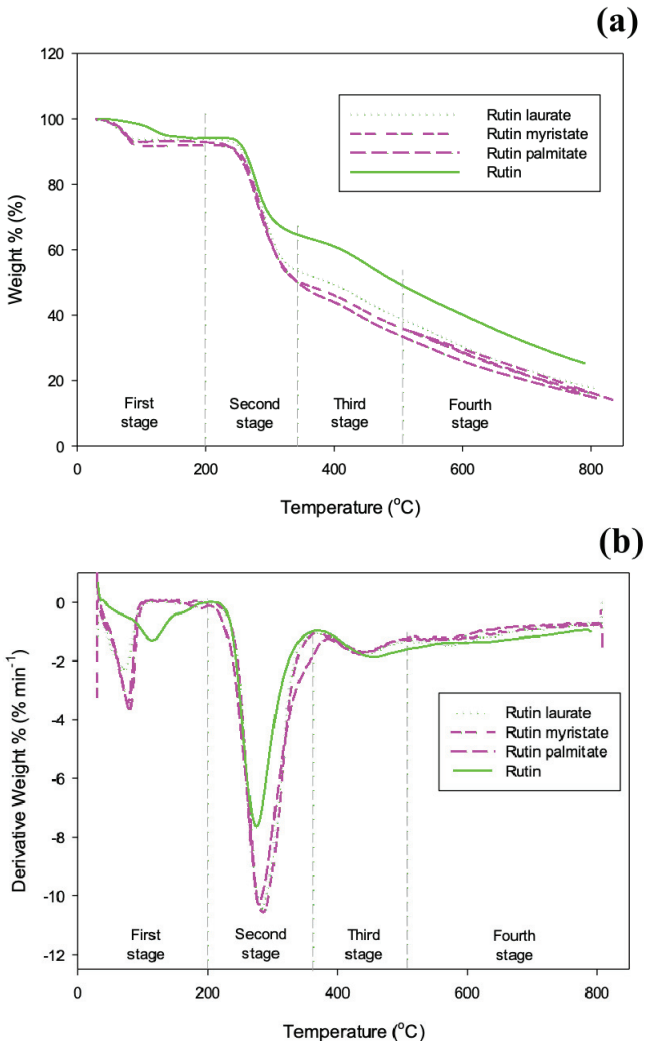

Fig. 1. Thermal decomposition analyses of rutin and its corresponding esters at heating rate of 15 °C min^{-1}: a) TG; b) DTG.

TABLE II. Stages and percentages of mass conversion in thermal degradation of rutin and its esters

Sample	T_i	T_{max}	Degradation stage				
	°C		First	Second	Third	Fourth	Total
Rutin	240.07	272.72	6.06	33.60	12.40	18.43	70.49
Rutin laurate (R-12)	220.19	282.05	5.89	41.74	13.70	20.50	81.87
Rutin myristate (R-14)	219.49	285.13	8.01	43.60	13.62	18.56	83.74
Rutin palmitate (R-16)	217.28	278.86	6.84	47.79	11.15	18.90	84.68

ond degradation stages from the DTG curves of rutin esters are much higher and sharper than for the rutin parent molecule (Fig.1b). The maximum temperature peak (T_{max}) is recorded in the second stage as drastic degradation of rutin and its esters occur. It was also reported that for temperatures above 100 °C, a sharp degradation of rutin was observed.[24] The onset of degradation temperature ($T_{initial}$) is used to indicate resistance to thermal degradation. Rutin is thermally stable up to 240 °C but its ester compounds exhibit lower $T_{initial}$ *viz.* 220, 219 and 217 °C for rutin laurate, rutin myristate and rutin palmitate, respectively (Table II). Thermal stability of rutin esters is lower than that of rutin parent molecule by 20 °C. Rutin is a type of flavonol glycosides consisting of quercetin and disaccharide rutinose (rhamnose and glucose). Based on isothermal profile, da Costa *et al.* reported that the presence of glycoside moieties in rutin alters its thermal degradation rate through lowering of degradation temperature compared to quercetin alone.[27] Relatively high temperature helps to promote the degradation of disaccharide substitution. Introduction of acyl donor to the glycone part of rutin culminates in a comparatively earlier onset of esters degradation. On the other hand, it can be seen that T_{max} for the studied rutin esters are higher than that of parent molecule, which corresponds to the decomposition of acyl donor group present in the esters (Table II).

The second degradation peaks of rutin esters are similar to pure rutin (200 to 390 °C). Major degradation of rutin is characterized by significant mass loss, *i.e.*, ~34 %. With the acyl substituents, mass loss of rutin esters in the second stage increases to 42, 44 and 48 %, respectively, due to longer carbon chain length. Longer chain fatty acid represents higher molecular weight of acyl donor group hence higher percentage of mass loss. Further mass loss occurs in the range of 333 to 498 °C when the evaporation of rutin and its esters come about (~18–20 %). This outcome implies that the degradation of rutin is influenced by temperature.[24] Finally, the compounds gradually decompose into final products at temperature above 498 °C. With longer acyl donor chain length, its decomposition leads to higher percentage of total degradation (Table II).

TG and DTG curves of rutin and its corresponding esters at heating rates of 5, 10, 15, 20 °C min^{-1} are shown in Figs. 2 and 3, respectively. For all samples, temperatures of recorded degradation stages increase progressively with higher heating rate. Maximum points of TG (Fig. 2) and minimum points of DTG curves (Fig. 3) shift towards higher temperatures. The observation is attributed to faster dissipation rate of heat at higher heating rate, consequently degradation occurs at comparatively higher temperature, thus the shift of TG curves to the right.

From the TG plot of rutin and its esters (Fig. 2), degradation starts at about 30 °C and proceed rapidly with increasing temperature until 270–280 °C. Then, weight loss decreases slowly until final temperature. The temperatures where 50

% weight loss ($T_{50\%}$) of rutin esters occur are lower than that of rutin parent molecule. At heating rates from 5 to 20 °C min^{-1}, $T_{50\%}$ for rutin shifts from 481.93 to 485.5 °C. For rutin laurate, it is about 106 °C lower than that for rutin (376.18 to 381.30 °C), while $T_{50\%}$ for rutin myristate (345.15 to 346.31 °C) and rutin palmitate (332.24 to 346.65 °C) are approximately 137 and 144 °C lower, respectively. In the temperature range of 795–808 °C, degradation of studied esters yields carbon residue approximately 20 % and below ($T_{80\%}$). In contrast, the final carbon residue from pure rutin sample is more than 20 %, corresponding to total weight loss of 22.97, 25.62, 28.99 and 29.46 % at the heating rates of 5, 10, 15 and 20 °C min^{-1}, respectively.

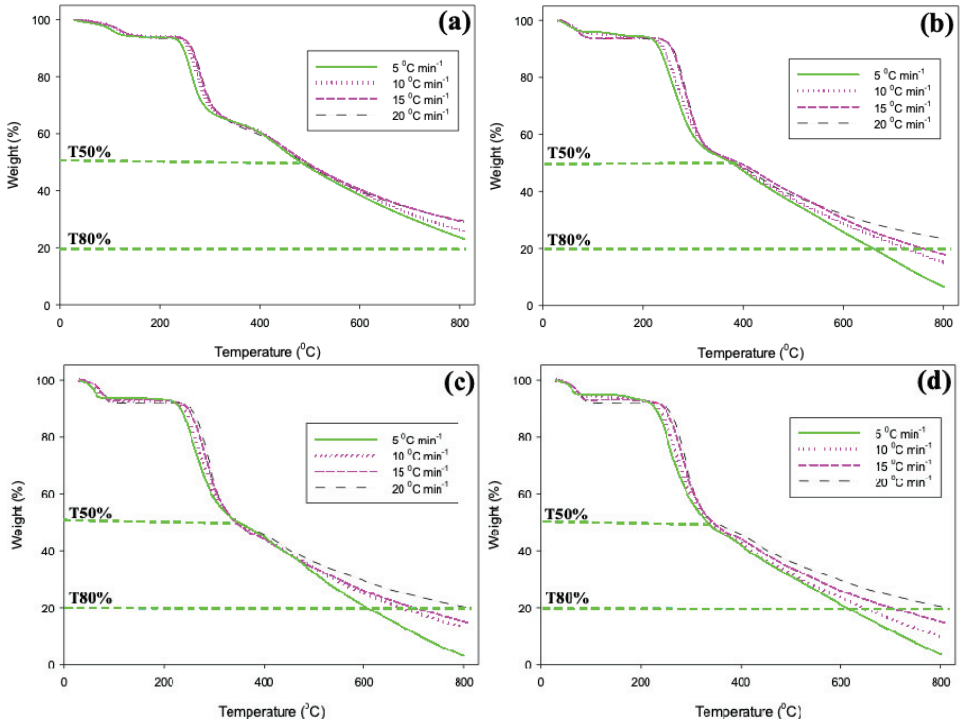

Fig. 2. TG curves of rutin and its corresponding esters at heating rates of 5, 10, 15 and 20 °C min^{-1} :a) rutin, b) rutin laurate, c) rutin myristate and d) rutin palmitate.

In the temperature range of 30–200 °C, DTG peaks of pure rutin are broader than its esters (Fig. 3a). The tailing of the rutin peaks become prevalent as the heating rate increases (indicated by an arrow). In the case of rutin esters (Fig. 3b––d), sharper peaks are observed at the early stage of degradation as heating rate increases. Temperature at the lowest point of the DTG curve indicates the temperature at the highest degradation rate. From Fig. 3, for heating rates of 5 to 20 °C min^{-1}, maximum mass loss rate increases rapidly, *viz.* –3.156 to –12.664 %

min^{-1} (259.88 to 274.57 °C), –2.579 to –14.62 % min^{-1} (270.65 to 283.98 °C), –2.705 to –14.88 % min^{-1} (270.04 to 288.33 °C) and –2.96 to –13.79 % min^{-1} (253.99 to 280.04 °C) for rutin, rutin laurate, rutin mysristate and rutin palmitate respectively.

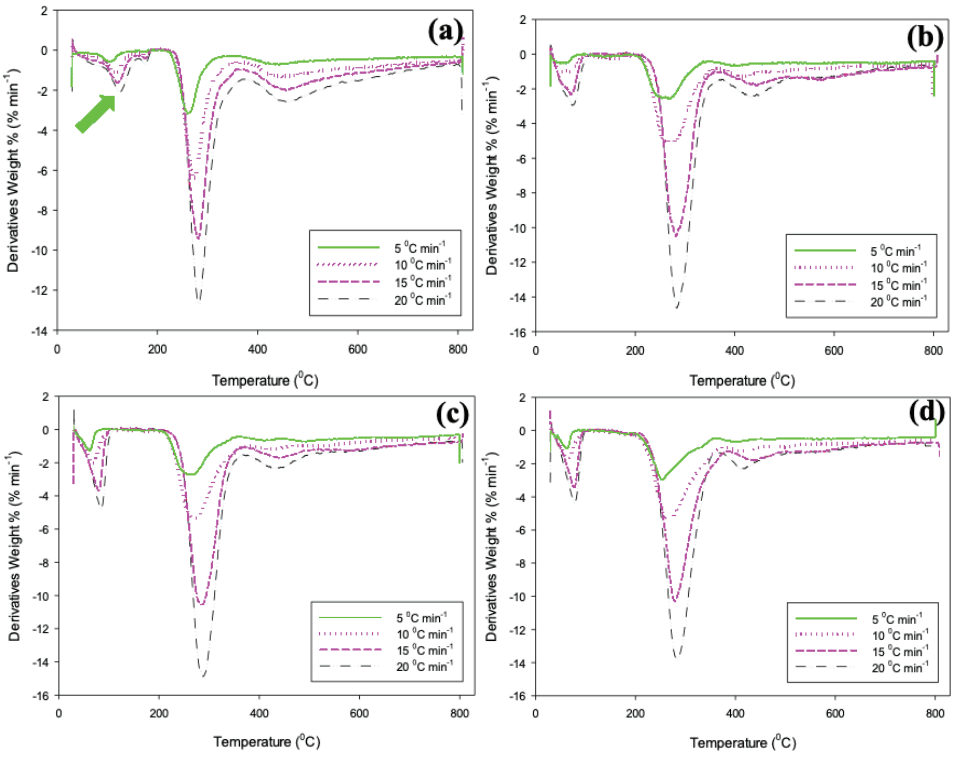

Fig. 3. DTG curves of rutin and its corresponding esters at heating rates of 5, 10, 15and 20 °C min^{-1}: a) rutin, b) rutin laurate, c) rutin myristate and d) rutin palmitate.

Activation energy in thermal degradation of rutin and its corresponding esters

Since the degradation of rutin and its corresponding esters involve multiple stages, the iso-conversional methods (model-free approach), namely KAS and FWO are preferred to calculate the kinetic parameters in order to better understand the process. The two methods allow for estimation of activation energy (E_a) as a function of conversion degree without the need to provide pre-assumption on the reaction function and reaction order. It allows for analysis of multi-step kinetics as a dependence of activation energy on conversion degree, subsequently making deductions with respect to the complexity of the process.

The regression lines based on KAS and FWO methods are presented in Figs. S-7 and S-8 of the Supplementary material, respectively. The regression lines of ln (β/T^2) *versus* $1/T$ for KAS method, and ln β *versus* $1/T$ for FWO method,

based on the same degree of conversion at different heating rates, allow for activation energy calculation from the slope. Excellent linear fitting of all data sets were achieved with coefficient of correlation, $R^2 > 0.98$. E_a values for thermal degradation of rutin and its corresponding esters were determined for mass conversion range of $0.05 < \alpha < 0.90$. The range spans the four separate degradation stages observed (Table II), for the temperature range 30 to 800 °C.

The activation energy (E_a) for thermal degradation of both rutin and its esters, when calculated using KAS and FWO methods, varies with conversion degree throughout the degradation process. Hence, it is obvious that thermal degradation of rutin and its esters proceed through a non-simple process. Nevertheless, for equal α studied, both methods yield E_a values with the high degree of agreement (Table III).

TABLE III. Activation energies calculated using KAS and FWO methods for thermal degradation of rutin and its esters

α	Sample	Kissinger–Akahira–Sunose (KAS) method		Flynn–Wall–Ozawa (FWO) method	
		E_a / kJ mol^{-1}	A	E_a / kJ mol^{-1}	A
0.05	Rutin	77	1.48×10^{10}	80	3.82×10^{10}
	Rutin laurate	81	2.25×10^{12}	82	4.13×10^{12}
	Rutin myristate	76	3.12×10^{11}	78	6.51×10^{11}
	Rutin palmitate	73	7.92×10^{10}	74	1.83×10^{11}
0.30	Rutin	205	5.23×10^{19}	203	3.88×10^{19}
	Rutin laurate	246	2.32×10^{23}	243	3.05×10^{16}
	Rutin myristate	176	2.93×10^{16}	176	4.51×10^{10}
	Rutin palmitate	110	1.82×10^{10}	113	1.37×10^{13}
0.60	Rutin	218	3.49×10^{15}	218	3.40×10^{15}
	Rutin laurate	178	1.34×10^{13}	180	2.11×10^{13}
	Rutin myristate	153	1.60×10^{11}	156	3.22×10^{11}
	Rutin palmitate	101	1.12×10^{7}	107	5.24×10^{7}
0.90	Rutin	224	1.38×10^{12}	228	2.45×10^{12}
	Rutin laurate	65	144307	77	78787
	Rutin myristate	66	62909	77	16028
	Rutin palmitate	67	52652	78	19297

From Table III, for each α, E_a calculated from both methods exhibit very similar trend with respect to the increase in the length of carbon chain of acyl donor with relative error less than 5 %, a considerably low hence tolerable error range.

At the first stage of degradation ($\alpha = 0.05$), rutin and its esters show comparable activation energies, *viz*. 73–81 kJ mol^{-1} for KAS method and 74–82 kJ mol^{-1} for FWO method (Table III). These values are in accord with the weight losses shown in Table II, attributable to loss of water molecules and evaporation of volatile compounds. For pure rutin, the E_a values calculated by both KAS and

FWO methods grew larger in magnitude throughout the progressive α, *i.e.*, 0.05 to 0.90, and increasing degradation temperature (*i.e.*, E_a 77 to 224 kJ mol^{-1} for KAS method; 80 to 228 kJ mol^{-1} for FWO method, Table III). The observed trend is in stark contrast to its corresponding esters where they exhibit a maximum in E_a when α = 0.30, before it decreases, and corroborated by both KAS and FWO methods. The observations implicitly identify distinct thermal degradation routes undergone by rutin and its corresponding esters, as most likely non-elementary. For α range from 0.60 to 0.90, E_a values for thermal degradation of pure rutin are consistently highest compared to its corresponding esters. E_a values for the latter increase from α = 0.05 to α = 0.30, and decrease steeply afterwards (Table III).

For all three rutin esters, highest E_a is at α = 0.30 as determined and agreed by both KAS and FWO methods (Table III). It is hypothesized that at α = 0.30, and coincided with the second DTG peak, the calculated E_a is minimal activation requirement for breaking of ester bond between acyl donor chain and rutin parent molecule. The E_a for decomposition of rutin ester to rutin and acyl donor fraction is suggested to depend upon the length of acyl donor carbon chain where E_a decreases with the increase in the carbon length of acyl moiety attached to rutin parent molecule, and it is clearly inferable from Table III with respect to α 0.30 to 0.60 as agreed by both KAS and FWO methods. It is proposed that the stable C–C distribution within rutin parent molecule is reduced as the carbon length of attached acyl moiety increases. The mean bond enthalpies in the aromatic rings of quercetin and its sugar moiety are much higher than that of rutin parent molecule bonded to aliphatic carbons. These results agreed with the roasting studies by Rohn *et al.*[28] They reported that thermal degradation behavior of several quercetin glycosides are subjected to the types and position of their sugar moieties. The main product is the aglycone quercetin which remains stable as thermal degradation progresses at 180 °C for 60 min. The E_a data obtained in this study, specifically in the α range of 0.30–0.60, also implied that the rutin esters studied may follow distinct mechanisms in their thermal degradation.

At α = 0.90, corresponding to the final degradation stage, the highest E_a value for rutin parent molecule is revealed by both KAS and FWO methods (224 and 228 kJ mol^{-1}, respectively). For the three rutin esters, the E_a values are in range of 65 to 67 kJ mol^{-1} obtained using KAS method, and comparably similar at 77 to 78 kJ mol^{-1} by FWO method. The E_a value of rutin is almost three times higher than those for its esters at α = 0.90, corresponding to the degradation of sugar moiety of the rutin. In contrast, significantly lower E_a values are determined for the three rutin esters, *i.e.*, the energy barrier to overcome in the internal chain breaking of separated acyl moiety during the final stage of degradation. These results corroborate with the almost equal observed mass loss 18–20 %

(Table II) for the three rutin esters studied. The findings made in this study agree with da Costa *et al.*[25]

Thermodynamic parameters of rutin and rutin esters

Thermodynamic parameters, while essential in providing insight into the nature of thermal degradation, are often overlooked for phytochemicals that include flavonoid compounds.[29] The thermodynamic parameters in the thermal degradation of rutin and its esters are summarized in Table IV.

TABLE IV. Thermodynamic parameters in thermal degradation of rutin and its esters at different conversion levels at the heating rate of 20 °C min^{-1}

α	Sample	Kissinger–Akahira–Sunose (KAS) Method			Flynn–Wall–Ozawa (FWO) method		
		ΔH kJ mol^{-1}	ΔG kJ mol^{-1}	ΔS J K^{-1} mol^{-1}	ΔH kJ mol^{-1}	ΔG kJ mol^{-1}	ΔS J K^{-1} mol^{-1}
0.05	Rutin	75	98	–60	76	97	–52
	Rutin laurate	78	84	–17	79	84	–12
	Rutin myristate	73	85	–34	75	85	–28
	Rutin palmitate	70	86	–45	72	85	–38
0.30	Rutin	200	135	119	199	135	117
	Rutin laurate	242	138	188	238	137	184
	Rutin myristate	171	140	57	171	139	57
	Rutin palmitate	105	140	–61	108	138	–54
0.60	Rutin	212	185	37	213	185	38
	Rutin laurate	172	178	–9	174	178	–5
	Rutin myristate	148	180	–46	151	179	–40
	Rutin palmitate	96	183	–125	102	180	–113
0.90	Rutin	217	245	–30	220	244	–26
	Rutin laurate	57	211	–163	68	258	–188
	Rutin myristate	58	208	–170	69	239	–182
	Rutin palmitate	60	211	–171	70	238	–180

The values of ΔH, ΔG and ΔS calculated at different conversion levels and the highest rate of the degradation occurrence. Positive ΔH indicates thermal degradation of rutin and its esters is endothermic (Table IV). These results corroborate the DSC results obtained by the other findings that show rutin samples exhibit endothermic events.[30,31] A comparable ΔH value for rutin is observed at α = 0.30 to 0.90 which maybe happen due to greater thermal resistance of the pure rutin molecule. It is suggested pyrolytic decomposition is mainly regulated by the stable C–C distribution. Hydrogen bonds and aromatic, π electron interactions develop between the rings A and C may influence the stabilization efficiency of the rutin. Lower value of ΔH for rutin esters corresponds to lower energy constraint for their thermal degradation relative to pure rutin. Lower values of ΔH are observed with longer acyl chain length. One plausible explan-

ation might be that during the pyrolysis process, after the weak bonds degraded (α = 0.05) and then aromatic, π electron interactions develop between the rings started to degrade accounted for the further increase in ΔH and activation energies. The whole pyrolysis is mainly controlled by 15-carbon flavone skeleton of flavonoid rutin and its intermediate products during pyrolysis. It is hypothesized that above 260 °C, degradation involves the saccharide moiety and it interferes with the stabilization reactions.[1] Disaccharides are temperature-sensitive, particularly during high-temperature processing. In this case, the degradation of the acylated saccharides become more profound with longer acyl chain length reflected by lower value of ΔH (α = 0.30 to 0.60). The long hydrocarbon chain allows less interactions to take place inside the aromatic rings, demanding less energy to break these bonds. At the highest degradation (α = 0.30), the variances in positive ΔH values of rutin esters are calculated at 67–71, 63–66 and 130–137 kJ mol^{-1} corresponding to differences between rutin laurate and rutin myristate, rutin myristate and rutin palmitate, rutin laurate and rutin palmitate respectively. The range shown is provided from calculation based on KAS and FWO methods (Table IV).

The Gibbs energy change (ΔG) values calculated for thermal degradation of rutin and its esters are positive, corresponding to a non-spontaneous and thermodynamically non-favorable process. At any specific α, negligible variation of ΔG between rutin and its esters are observed. For all studied compounds, the ΔG values increase with temperature. At the time of this report, the ΔG values for pyrolysis of crystalline, different single-type flavonoid esters are yet to be reported. Possibly related are ΔG values estimated for thermal degradation of total flavonoid compound (TFC) in sweet cherries extract ranging 86–105 kJ mol^{-1}.[32]

In terms of entropy change (ΔS, Table IV), rutin parent compound shows positive ΔS indicative of its tendency towards energy and matter dispersal. Conversely, acylated rutins show transition from positive to negative values of ΔS, which reflect less tendency towards energy and matter dispersal for them. It is inferred that the acylation of rutin results in ester compounds that are not likely to be progressing towards a state of disorder. Reduced energy is needed as the compounds adopt more ordered structures.

CONCLUSION

Analyses of activation energy as a function of conversion degree, alongside thermodynamic parameters in the pyrolysis of rutin and its fatty acid esters filled an important void in the literature, and yield useful insights to potential product processing and development routes. Significant variations in activation energies were seen with conversion levels for rutin and its esters ranging from 65 to 246 kJ mol^{-1}. The ΔH (60 to 242 kJ mol^{-1}) and ΔG (84 to 245 kJ mol^{-1}) values for all compounds were positive, indicating endothermic and non-spontaneous nature

of pyrolysis. Δ*S* shows significant variation with conversion levels ranging from –188 to 180 J K^{-1} mol^{-1}. This clearly represents complex chemistry of thermal conversion with reactions of widely varying kinetic character occurring at different stages of conversion.

SUPPLEMENTARY MATERIAL

Additional data and information are available electronically at the pages of journal website: https://www.shd-pub.org.rs/index.php/JSCS/article/view/12453, or from the corresponding author on request.

Acknowledgements. The authors acknowledged research funding from Universiti Malaya, Malaysia (Grant No. ST072-2021) and MAHSA University (Grant No. RP206-12/23).

ИЗВОД

ТЕРМОХЕМИЈА ПИРОЛИЗОВАНОГ РУТИНА И ЊЕГОВИХ ЕСТАРА ПРИПРЕМЉЕНИХ ЈЕДНОСТАВНИМ БИОКАТАЛИТИЧКИМ ПУТЕМ

NURUL NADIAH ABD RAZAK[1,2] и MOHAMAD SUFFIAN MOHAMAD ANNUAR[3]

[1]Centre for Foundation Studies in Science, Universiti Malaya, 50603 Kuala Lumpur, Malaysia, [2]School of Bioscience, Faculty of Pharmacy and Biomedical Sciences, MAHSA University, Bandar Saujana Putra, Jenjarom, Selangor, Malaysia and [3]Institute of Biological Sciences, Faculty of Science, Universiti Malaya, 50603 Kuala Lumpur, Malaysia

Истраживана је пиролиза кверцетин-3-*O*-рутинозида или рутина, и његових естара. Пречишћени узорци естара су припремљени липазом-катализованом естерификацијом полазног флавоноида, тј. рутина, користећи ацил доноре са различитом дужином угљеничног ланца. Дифракција X-зрака је открила присуство кристалиничних пикова код естара рутина. Активационе енергије деградације (E_a) као функције степена конверзије одређене су методама Kissinger–Akahira–Sunose и Flynn–Wall–Ozawa, са узајамно подржавајућим резултатима. Неподударање у E_a имплицира различите путеве термалне деградације. За сва испитивана једињења, деградација није спонтан процес. Присуство ацил структурних елемената и дужина њихових ланаца угљеника дискутовано је у односу на термодеградационе профиле, E_a и промена ентропије (ΔS) и енталпије (ΔH) при пиролизи.

(Примљено 24. јуна, ревидирано 27. септембра, прихваћено 2. јануара 2024)

REFERENCES

1. B. Kirschweng, D. M. Tilinger, B. Hégely, G. Samu, D. Tátraaljai, E. Földes, B. Pukánszky, *Eur. Polym. J.* **103** (2018) 228 (https://doi.org/10.1016/j.eurpolymj.2018.04.016)
2. A. M. Mahmoud, *Exp. Toxicol. Pathol.* **64** (2012) 783 (https://doi.org/10.1016/j.etp.2011.01.016)
3. W. Lee, S. K. Ku, J. S. Bae, *Food Chem. Toxicol*. **50** (2012) 3048 (https://doi.org/10.1016/j.fct.2012.06.013)
4. D. S Kim, S. B Lim, *Prev. Nutr. Food Sci.* **22** (2017) 131 (https://doi.org/10.3746/pnf.2017.22.2.131)
5. A. Hunyadi, A. Martins, T. J. Hsieh, A. Seres, I. Zupkó, *PLoS ONE* (2012) (https://doi.org/10.1371/journal.pone.0050619)

6. J. P. Lin, J. S. Yang, J. J. Lin, K. C. Lai, H. F. Lu, C. Y. Ma, R. S. C. Wu, K. C. Wu, F. S. Chueh, W. G. Wood, J. G. Chung, *Environ. Toxicol*. **27** (2012) 480 (https://doi.org/10.1002/tox.20662)
7. R. Mauludin, R. H. Müller, C. M. Keck, *Int. J. Pharm.* **370** (2009) 202 (https://doi.org/10.1016/j.ijpharm.2008.11.029)
8. L. Chebil, C. Humeau, A. Falcimaigne, J. M. Engasser, M. Ghoul, *Process Biochem*. **41** (2006) 2237 (https://doi.org/10.1016/j.procbio.2006.05.027)
9. J. Viskupicova, M. Ondrejovic, T. Maliar, in *Biochemistry*, D. Ekinci, Ed., InTech Europe, Rijeka, 2021, p. 263 (https://doi.org/10.5772/34174)
10. M. E. M. de Araújo, Y. E. Franco, M. C. Messias, G. B. Longato, J. A. Pamphile, P. D. O. Carvalho, *Planta Med*. **83** (2017) 7 (https://doi.org/10.1055/s-0042-118883)
11. J. Viskupicova, M . Danihelova, M. Ondrejovic, T. Liptaj, E. Sturdik, *Food Chem.* **123** (2010) 45 (https://doi.org/10.1016/j.foodchem.2010.03.125)
12. B. Mbatia, S. S. Kaki, B. Mattiasson, F. Mulaa, P. Adlercreutz, *J. Agric. Food Chem.* **59** (2011) 7021 (https://doi.org/10.1021/jf200867r)
13. A. D. M. Sørensen, L. K. Petersen, S. de Diego, N. S. Nielsen, B. M. Lue, Z. Yang, X. Xu, C. Jacobsen, *Eur. J. Lipid Sci. Tech.* **114** (2012) 434 (https://doi.org/10.1002/ejlt.201100354)
14. B. M. Lue, N. S. Nielsen, C. Jacobsen, L. Hellgren, Z. Guo, X. Xu, *Food Chem.* **123** (2010) 221 (https://doi.org/10.1016/j.foodchem.2010.04.009)
15. J. Viskupicova, M. Majekova, L. Horakova, *J. Muscle Res. Cell. M.* **36** (2015) 183 (https://doi.org/10.1007/s10974-014-9402-0)
16. G. Kodelia, K. Athanasiou, F. N. Kolisis, *Appl. Biochem. Biotech.* **44** (1994) 205 (https://doi.org/10.1007/BF02779657)
17. F. Mellou, H. Loutrari, H. Stamatis, C. Roussos, F. N. Kolisis, *Process Biochem.* **41** (2006) 2029 (https://doi.org/10.1016/j.procbio.2006.05.002)
18. M. I. Cardona, N. M. N. Le, S. Zaichik, D. M. Aragón, A. Bernkop-Schnürch, *Int. J. Pharm.* **562** (2019) 180 (https://doi.org/10.1016/j.ijpharm.2019.03.036)
19. N. N. A. Razak, M. S. M. Annuar, *Ind. Eng. Chem. Res.* **54** (2015) 5604 (https://doi.org/10.1021/acs.iecr.5b00996)
20. A. Kontogianni, V. Skouridou, V. Sereti, H. Stamatis, F. N. Kolisis, *Eur. J. Lipid Sci. Technol.* ***103*** (2010) 655 (https://doi.org/10.1002/1438-9312(200110)103:10<655::AID-EJLT655>3.0.CO;2-X)
21. M. Ardhaoui, A Falcimaigne, S. Ognier, J. M. Engasser, P. Moussou, G. Pauly, M. Ghoul, *J. Biotechnol.* **110** (2004) 265 (https://doi.org/10.1016/j.jbiotec.2004.03.003)
22. M. Şamlı, O. Bayraktar, F. Korel, *J. Incl. Phenom. Macromol.* **80** (2014) 37 (https://doi.org/10.1007/s10847-014-0396-4)
23. S. Sun, Y. Jin, Y. Hong, Z. Gu, L. Cheng, L. Zhaofeng, L. Caiming. *Food Hydrocoll.* **110** (2021) 106224 (https://doi.org/10.1016/j.foodhyd.2020.106224)
24. H. Chaaban, I. Ioannou, L. Chebil, M. Slimane, C. Gérardin, C. Paris, C. Charbonnel, L. Chekir, M. Ghoul, *J. Food Process. Preserv.* **41** (2017) e13203 (https://doi.org/10.1111/jfpp.13203)
25. Ç. Kadakal, T. Duman, R. Ekinci. *Food Sci. Technol.* ***38*** (2017) 667-673 (https://doi.org/10.1590/1678-457X.11417)
26. Ç. Kadakal, T. Duman, *Pamukkale Üniversitesi Mühendislik Bilimleri Dergisi* **24** (2018) 1370-1375 (https://doi.org/10.5505/pajes.2017.03779)
27. E. M. da Costa, J. M. Barbosa Filho, T. G. do Nascimento, R. O. Macêdo, *Thermochim. Acta* **392** (2002) 79 (https://doi.org/10.1016/S0040-6031(02)00087-4)

28. S. Rohn, N. Buchner, G. Driemel, M. Rauser, L.W. Kroh, *J. Agric. Food Chem.* **55** (2007) 1568 (https://doi.org/10.1021/jf063221i)
29. N. Stănciuc, G. Râpeanu, in *Non-Alcoholic Beverages*, A. Grumezescu, A.M. Holban, Eds., Woodhead Publishing, Sawston, 2019, p. 407 (ISBN 9780128152706)
30. D. C. de Medeiros, S. S. Mizokami, N. Sfeir, S. R. Georgetti, A. Urbano, R. Casagrande, W. A. Verri, M. M. Baracat, *ACS Omega* **4** (2019) 1221-1227 (https://doi.org/10.1021/acsomega.8b02868)
31. M. K. Remanan, F. Zhu, *Food Chem.* **353** (2021) 128534 (https://doi.org/10.1016/j.foodchem.2020.128534)
32. M. Turturică, N. Stănciuc, G. Bahrim, G. Râpeanu, *Food Bioprocess Tech.* **9** (2016) 1706 (https://doi.org/10.1007/s11947-016-1753-7).